Available online at www.sciencedirect.com
SCIENCE DIRECT®
Biochemical Pharmacology 67 (2004) 1689–1700
Biochemical Pharmacology
www.elsevier.com/locate/biochempharm

Combination treatment of glioblastoma multiforme cell lines with the anti-malarial artesunate and the epidermal growth factor receptor tyrosine kinase inhibitor OSI-774

Thomas Efferth[a,*], Tzutzuy Ramirez[b], Erich Gebhart[c], Marc-Eric Halatsch[d]

[a]*Center for Molecular Biology, University of Heidelberg, Im Neuenheimer Feld 282, Heidelberg 69120, Germany*
[b]*Unidad de Investigacion Biomedica en Cancer, Instituto de Investigationes Biomedicas—Instituto Nacional de Cancerologia, Mexico DF, Mexico*
[c]*Institute for Human Genetics, University of Erlangen-Nürnberg, Erlangen, Germany*
[d]*Department of Neurosurgery, University of Göttingen, Göttingen, Germany*

Received 3 November 2003; accepted 23 December 2003

Abstract

New drugs and combination modalities for otherwise non-responsive brain tumors are urgently required. The anti-malarial artesunate (ART) and the EGFR tyrosine kinase inhibitor OSI-774 reveal profound cytotoxic activity. The effectiveness of a combination treatment and the underlying molecular determinants of cellular response are unknown. In the present investigation, we studied ART and OSI-774 in glioblastoma multiforme (GBM) cell lines. Supra-additive inhibition of cell growth was observed in U-87MG.ΔEGFR cells transduced with a deletion-mutant constitutively active EGFR gene, while additive effects were present in cells transduced with wild-type EGFR (U-87MG.WT-2N), kinase-deficient EGFR (U-87MG.DK-2N), mock vector controls (U-87MG.LUX), or non-transduced parental U-87MG cells. Among nine other non-transduced GBM cell lines, supra-additive effects were found in two cell lines (G-210GM, G-599GM), while ART and OSI-774 acted in an additive manner in the other seven cell lines (G-211GM, G-750GM, G-1163GM, G-1187GM, G-1265GM, G-1301GM, and G-1408GM). Sub-additive or antagonistic effects were not observed. Genomic gains and losses of genetic material in the non-transduced cell lines as assessed by comparative genomic hybridization were correlated with the IC_{50} values for ART and OSI-774 and subsequently subjected to hierarchical cluster analysis and cluster image mapping. A genomic profile of imbalances was detected that predicted cellular response to ART and OSI-774. The genes located at the genomic imbalances of interest may serve as candidate resistance genes of GBM cells towards ART and OSI-774. In conclusion, the combination treatment of ART and OSI-774 resulted in an increased growth inhibition of GBM cell lines as compared to each drug alone.

Keywords: Artesunate; Epidermal growth factor receptor; Comparative genomic hybridization; Glioblastoma multiforme; Hierarchical cluster analysis; Small molecule inhibitor

1. Introduction

Current standard chemotherapies for cancer are still inadequate regarding drug resistance and toxicity. As a consequence of dose-limiting toxicity, concentrations necessary to kill resistant subpopulations of tumor cells can frequently not be achieved, leading to the ultimate failure of chemotherapy. Faced with these major limitations of current cancer chemotherapy, there is an urgent requirement for new drugs and combination treatment modalities with acceptable toxicity profiles and activity against otherwise non-responsive tumors.

The human epidermal growth factor receptor (EGFR, HER1) represents a valuable target for the development of novel therapeutic strategies. A specific deletion-mutation in the *EGFR* gene increases cellular tumorigenicity [1], and amplification and/or over-expression of the *EGFR* is of prognostic relevance for many types of solid tumors including glioblastoma multiforme (GBM) [2]. Upon ligand binding and homo- or heterodimerization with HER2, another member of the *EGFR* gene family, the intracellular tyrosine kinase domain is activated. EGFR activation can

Abbreviations: ART, artesunate; EGFR, epidermal growth factor receptor; GBM, glioblastoma multiforme; IC_{50}, inhibition concentration 50%

* Corresponding author. Tel.: +49-6221-546790; fax: +49-6221-653195.
E-mail address: thomas.efferth@web.de (T. Efferth).

0006-2952/$ – see front matter © 2004 Elsevier Inc. All rights reserved.
doi:10.1016/j.bcp.2003.12.035

stimulate the Raf/Mek/Erk, the phosphatidylinositol 3-kinase (PI3K)/phosphoinositide-dependent kinase-1 (PDK1)/Akt, and the phospholipase Cγ (PLCγ)/protein kinase C (PKC) signal transduction pathways [3]. The activation of EGFR-coupled signaling routes drive mitogenic and other cancer-promoting processes, e.g., proliferation, invasion, angiogenesis, cell motility, cell adhesion, inhibition of apoptosis, and the development of drug resistance. The deregulated activation of the receptor's tyrosine kinase activity, e.g., by gene amplification or deletions throughout the ligand-binding domain in exons 2–7, is critical for the malignant transformation of cells.

Since these functional and structural alterations have been strongly implicated in increased cellular proliferation and tumorigenesis, decreased apoptosis, and poor prognosis, several strategies, including monoclonal antibodies, immunotoxin conjugates, anti-sense oligonucleotides, siRNA, and ribozymes, have attempted to ultimately intercept cellular effects mediated by quantitatively and qualitatively aberrant EGFR [4]. Small molecules, e.g., ZD1839, OSI-774, PKI-166, PD158780, AG1478, CGP59326, and CI-1033, either interfere with the signal-transducing tyrosine phosphorylation activity or enhance ubiquitination and endocytotic degradation of EGFR. A salient feature of EGFR inhibitors is that they improve tumor cell killing if applied in combination with standard antineoplastic agents [5,6]. Hence, such combination treatment approaches may provide novel solutions for more effective treatments of human cancers.

OSI-774 is a quinazoline that inhibits the tyrosine kinase activity of EGFR and induces apoptosis and cell cycle arrest [7,8]. In a recent study, we have shown that the ability of GBM cell lines to induce EGFR mRNA expression after exposure to OSI-774 was associated with decreased susceptibility to the anti-tumorigenic effect of OSI-774 as a cellular effort to counteract functional EGFR inhibition by this drug [9].

Another novel compound with profound cytotoxicity against tumor cells is ART. This is a semisynthetic derivative of artemisinin, the active principle of *Artemisia annua* L. Though initially described as an anti-malarial drug, ART proved to be active in 55 cell lines of the National Cancer Institute (N.C.I.), USA [10]. Mining the N.C.I.'s database for the mRNA expression microarray data for 465 genes showed that *EGFR* gene expression correlated inversely with the cellular sensitivity to ART, indicating that *EGFR* is a determinant of cellular response to ART [11].

While both drugs are well described concerning their activity against tumor cells, nothing is known about the effectiveness of a combination treatment and the underlying molecular determinants of cellular response. In the present investigation, we have analyzed the small molecule EGFR tyrosine kinase inhibitor OSI-774 in combination with ART in a panel of 14 GBM cell lines, in order to identify molecular factors that may determine the cellular response to this combination treatment. Therefore, ART was tested in combination with OSI-774 in GBM cell lines transduced with expression vectors carrying either wild-type or deletion-mutant *EGFR* cDNAs as well as in a panel of GBM cell lines with varying degrees of inherent *EGFR* expression. Furthermore, the comparative genomic hybridization technique was used to identify genomic imbalances that correlated with the IC_{50} values of GBM cell lines for ART and OSI-774. Finally, a profile of genomic aberrations has been identified by hierarchical cluster analysis that predicted sensitivity or resistance of GBM cell lines to the combination of ART and OSI-774.

2. Material and methods

2.1. Drugs

OSI-774 ([6,7-bis(2-methoxy-ethoxy)quinazoline-4-yl]-(3-ethylphenyl)amine) was kindly provided by OSI Pharmaceuticals. ART was obtained from Saokim Ltd.

2.2. Cell lines

The establishment of the parental human GBM cell line U-87MG and its derivatives which over-express exogenous wild-type epidermal growth factor receptor (U-87MG.WT-2N), tyrosine kinase-deficient EGFR (U-87MG.DK-2N), constitutively active EGFR with a genomic deletion of exons 2–7 (U-87MG.ΔEGFR), or control expression vector (U-87MG.LUX), respectively, has been described elsewhere [12]. The cell lines were kindly provided by Dr. W.K. Cavenee (Ludwig Institute for Cancer Research, San Diego, CA, USA). Cell culture conditions of these cell lines were as described [13].

Nine established GBM cell lines derived from histopathologically confirmed neurosurgical specimens obtained in the Department for Neurosurgery, University of Göttingen, Germany, were maintained in RPMI 1640 medium (BioWhittaker) supplemented with 10% heat-inactivated fetal calf serum and incubated in a humidified 5% CO_2 atmosphere at 37 °C. Medium was exchanged twice weekly, and cells were passaged upon reaching subconfluence. At the beginning of the study, all cell lines were beyond their 20th passage.

2.3. Growth inhibition assay

The in vitro response to cytostatic drugs was evaluated by means of a growth inhibition assay. Aliquots of 5×10^3 cells/ml were seeded in culture medium, and drugs were added at different concentrations. Cells were counted 10 days after seeding. These growth curves represent the net outcome of cell proliferation and cell death. Cell numbers were quantified each in eight independent determinations. To detect additive or synergistic effects in combination treatments, OSI-774 and ART were applied

at 50% isodoses and plotted in isobolograms as previously described [14,15].

2.4. Colony forming assay

Tumor cells (2×10^3 cells/ml) were seeded in 60-mm dishes. After changing the medium two days later, treatment with different drug concentrations was initiated. One week later, the colonies that grew from the surviving cells were fixed in ethanol acetic acid (3:1), stained with 0.1% toluidine blue, and counted.

2.5. Comparative genomic hybridization

DNA was extracted using TriStar™ reagent (Hybaid) and subjected to comparative genomic hybridization (CGH) on metaphase chromosomes of normal peripheral lymphocytes prepared on slides. The CGH protocol used has been previously described in detail [16]. The validity of this method has been proven on a series of leukemia cases [17,18]. Briefly, 500 ng tumor DNA and 500 ng normal DNA were labeled with biotin and digoxigenin, respectively, by nick translation (Roche Diagnostics). The probe mixture of 500 ng tumor DNA, 500 ng normal DNA, 20 μg Cot-1 DNA (GIBCO BRL Life Technologies) and 10 μg herring testis DNA (Sigma-Aldrich) was denatured in 50% formamide/20% dextran sulphate/2× SSC/50 mM sodium phosphate buffer for 3 min at 75 °C and pre-annealed at 37 °C for 20 min. The probe mixture was hybridized to a normal lymphocyte metaphase slides denatured in 70% formamide/2× SSC/sodium phosphate buffer, and sealed with cover slides and rubber cement. The slides were incubated at 37 °C for three days in a humidified chamber. For fluorescence detection, the slides were stained with avidin-fluorescein isothiocyanate (Vector Laboratories) and anti-digoxigenin-rhodamine (Roche Diagnostics), followed by counter-staining with 4′,6-diamidino-2-phenylindole dihydrochloride (DAPI). The slides were mounted in 20 μl anti-fade solution (Vectashields, Vector Laboratories) and evaluated using a fluorescence microscope (Axioplan Zeiss) equipped with a CCD camera (IMAC S30) and the ISIS 3 software (MetaSystems). Gains or losses of genetic material were deemed as significant by the evaluation software if fluorescence ratio borderline values of 1.2 and 0.8 were not reached or exceeded, respectively. Twenty karyotypes were analyzed per experiment.

2.6. Statistical analyses

Hierarchical cluster analysis is an explorative statistical method which groups seemingly heterogeneous objects into clusters of homogeneous objects. Objects are classified by calculation of distances according to the closeness of inter-individual distances. All objects are assembled into a cluster tree (dendrogram). The merging of objects with similar features leads to the formation of a cluster, where the length of the branch indicates the degree of relation. The procedure continues to aggregate clusters until there is only one. The distance of subordinate clusters to a superior cluster represents a criterion for the closeness of clusters as well as for the affiliation of single objects to clusters. Thus, objects with tightly related features appear together, while the distance in the cluster tree increases with progressive dissimilarity. The applicability of cluster tree models for comparative genomic hybridization data has been demonstrated previously [19,20]. Cluster analyses applying the complete-linkage method were done by means of the WinSTAT program (Kalmia). Missing values were automatically omitted by the program, and the closeness of two joined objects was calculated by the number of data points they contained. In order to calculate distances of all variables included in the analysis, the program automatically standardizes the variables by transforming the data with mean = 0 and variance = 1. Standard statistical tests (Wilcoxon test, χ^2 test) were used as implements of the WinSTAT program.

3. Results

3.1. Growth inhibition assays

As a starting point, growth inhibition after exposure to OSI-774 has been determined in all glioblastoma cell lines investigated. OSI-774 has been applied in a concentration range from 0.1 to 30 μM to U-87MG.ΔEGFR cells transduced with a deletion-mutant *EGFR* and U-87MG control cells (Fig. 1a). The IC_{50} values for OSI-774 calculated from the dose-response curves were 1.6 μM for U-87MG.ΔEGFR and 8.6 μM U-87MG cells. Hence, U-87MG.ΔEGFR cells were 5.5-fold more sensitive to OSI-774 than U-87MG cells. These dose-response curves demonstrate that a single concentration of 1 μM OSI-774 is sufficient to differentiate between both cell lines. Further experiments with all other cell lines were, therefore, performed with this concentration of OSI-774 (1 μM). The left part of Fig. 1b represents the cell growth of all cell lines after exposure to 1 μM OSI-774. The cell growth was inhibited to a different extent in the cell lines analyzed. As compared to untreated control cells, the growth of U-87MG.ΔEGFR cells was 61.7% and of U-87MG.WT-2N cells 66.2% after exposure to 1 μM OSI-774, whereas the growth of U-87MG.DK-2N, U-87MG.LUX, and U-87MG cells was in a range of 84.5 and 98.2%. The growth of the non-transduced cell line panel after addition of 1 μM OSI-774 ranged from 76.6% (G-599GM) to 101.8% (G-1265GM) (Fig. 1b).

A concentration of 1 μM OSI-774 was also used for the combination treatment with ART which was applied in a concentration range of 0.01–30 μg/ml (0.026–78 μM). As depicted in Figs. 2 and 3, the ART-induced cell growth inhibition expressed as percentage of cell growth of

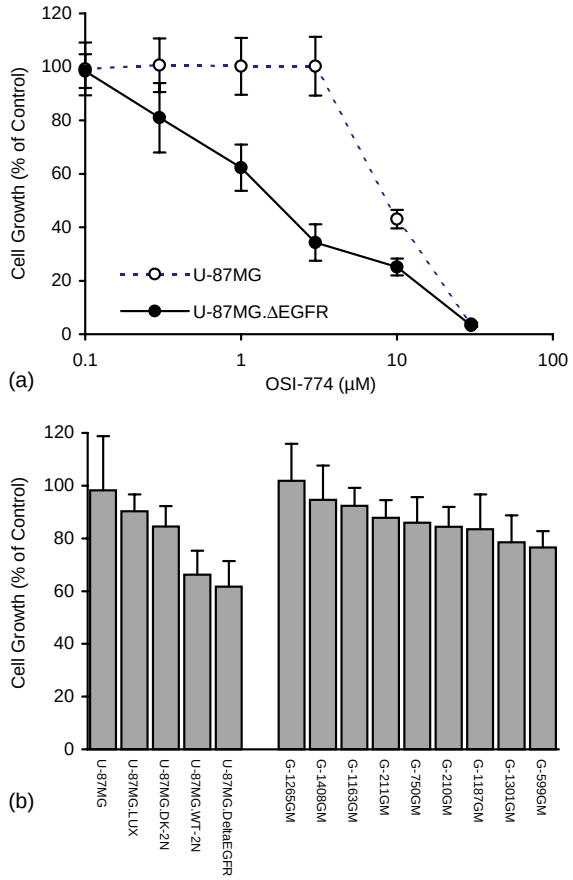

Fig. 1. Treatment responses of GBM cell lines with OSI-774 assessed by the growth inhibition assay. (a) Dose–response curves of U-87MG and U-87MG.ΔEGFR cells after exposure to 0.1–10 μM OSI-774. (b) Treatment of transduced and non-transduced GBM cell lines with 1 μM OSI-774. Each data point or bar represents mean ± S.D. of eight measurements.

untreated control cells varied considerably between the cell lines. The values of growth inhibition for 1 μM OSI-774 alone were set as 100%, and cell growth rates under the combination treatment of ART and OSI-774 were related to these control values. This means that a strictly additive effect of both drugs appears as an overlapping dose-response curve compared to treatment with ART alone, while supra-additive effects of ART plus OSI-774 are visible as a curve below that for ART alone. As depicted in Fig. 2, the combination of ART plus OSI-774 led to a strong increase of growth inhibition compared to ART alone in U-87MG.ΔEGFR cells but not in U-87MG.WT-2N, U-87MG.DK-2N, U-87MG.LUX, or U-87MG cells. The degree of increase of inhibition by ART plus OSI-774 compared to ART alone was 25-fold in U-87MG.ΔEGFR cells, while it ranged from 1.0- to 14.1-fold in the other U-87MG cell lines (Table 1). Interestingly, the response of U-87MG.ΔEGFR cells to ART or OSI-774 was different. While these cells were highly sensitive to OSI-774 (Fig. 1a), they were resistant to ART (Table 1).

Among nine non-transduced GBM cell lines, the G-210GM and G-599GM cell lines showed increased growth inhibition rates by the combination of both drugs with multiplicities of 14.1- and 7.0-fold, respectively, compared to treatment with ART alone (Fig. 3, Table 1), indicating supra-additive effects. ART plus OSI-774 caused modestly increased growth inhibitions compared to ART alone in G-750GM and G-1408GM cell lines (1.6- and 2.3-fold, respectively). The other five cell lines displayed no or only minimal increases of growth inhibition (<1.5-fold), indicating that ART plus OSI-774 act strictly additive in these cell lines. Sub-additive or antagonistic effects were not observed at all.

3.2. Isobolographic analyses

These observations were then confirmed using isobolographic analyses. We used the G-599GM cell line for these experiments, because it showed a supra-additive modulation of ART by OSI-774 compared to ART alone in growth inhibition assays. As a first step, OSI-774 alone was applied in different concentrations. The IC_{50} value calculated from this dose-response curve was 1.3 μM. The IC_{50} value for ART alone was 4.2 μM in G-599GM cells (Table 1). As a second step, both drugs were then applied together in concentrations of 20, 40, 60, and 80% of the corresponding IC_{50} values of each drug alone. Fig. 4a shows that the dose-dependent inhibition of ART alone was enhanced by addition of OSI-774. The increase in growth inhibition rose with serially increasing OSI-774 concentrations. Plotting of the data against OSI-774 at the *x*-axis (Fig. 4b) indicated that the increasing IC_{50} fractions of ART enhanced the growth inhibitory activity of OSI-774. Plotting of the combination treatment IC_{50} values of OSI-774 against ART revealed a supra-additive inhibition of cell growth (Fig. 4c). The results obtained by means of the growth inhibition assay were then scrutinized using a

Table 1
IC_{50} values of GBM cell lines after treatment with ART and OSI-774 in growth inhibition assays

Cell lines	IC_{50} values (μM)		Modulation index[a]
	ART alone	ART + OSI-774	
U-87MG	2.0	2.1	1.0
U-87MG.LUX	2.3	1.9	1.2
U-87MG.DK-2N	3.0	2.1	1.4
U-87MG.WT-2N	4.9	3.7	1.3
U-87MG.ΔEGFR	11.5	0.5	25.0
G-211GM	1.5	1.5	1.0
G-599GM	4.2	0.6	7.0
G-1301GM	4.2	3.8	1.1
G-750GM	5.2	3.3	1.6
G-1187GM	6.7	5.9	1.1
G-1408GM	7.5	3.2	2.3
G-210GM	15.5	1.1	14.1
G-1265GM	8.5	7.0	1.2
G-1163GM	18.8	15.8	1.2

[a] IC_{50} for ART alone divided by IC_{50} for ART + OSI-774.

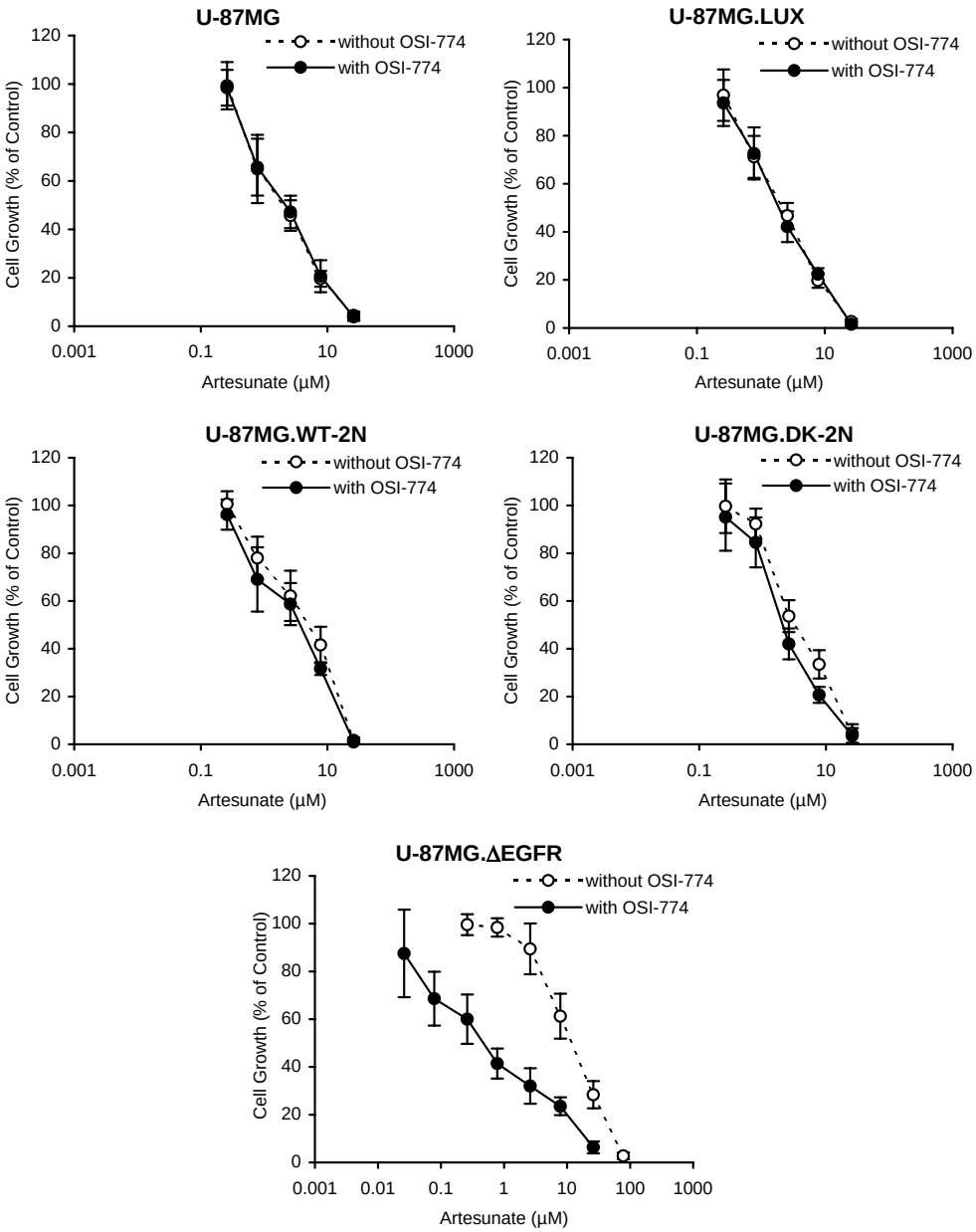

Fig. 2. Combination treatment of various *EGFR*-transduced GBM cell lines with ART and OSI-774 assessed by the growth inhibition assay. Cell growth inhibition by ART alone (open circles) or by ART plus OSI-774 (1 μM) (closed circles) is expressed as percentage of controls. U-87MG.ΔEGFR cells, transduced with deletion-mutant *EGFR*; U-87MG.DK-2N transduced cells with tyrosine kinase deficient *EGFR*; U-87MG.WT-2N, cells transduced with wild-type *EGFR*; U-87MG.LUX, cells transduced with expression vector only; U-87MG, non-transduced parental cells. Data represent mean ± S.D. of eight measurements.

second independent test method. As shown in Fig. 4c, comparable results were found by the colony forming assay.

3.3. Comparative genomic hybridization and hierarchical cluster analysis

The genomic imbalances (gains or losses of genetic material) in the non-transduced GBM cell lines have been described by our group [21]. In the present investigation, all genomic aberrations detected in these cell lines were correlated with the IC_{50} values for ART and OSI-774 by means of the Wilcoxon test. For this reason, the cell lines were grouped as being positive or negative for a given genomic imbalance. Those imbalances which showed a relationship to cellular drug response at a significance level of $P < 0.09$ were subjected to subsequent hierarchical cluster analysis. Relationships with a significance level of $P > 0.09$ were excluded from hierarchical cluster analysis. Representative chromosomal profiles of genomic hybridizations harboring these imbalances are shown in Fig. 5. Enhancements or amplifications of genetic material are marked by a bar to the right and losses by a bar to the left in each chromosomal graph.

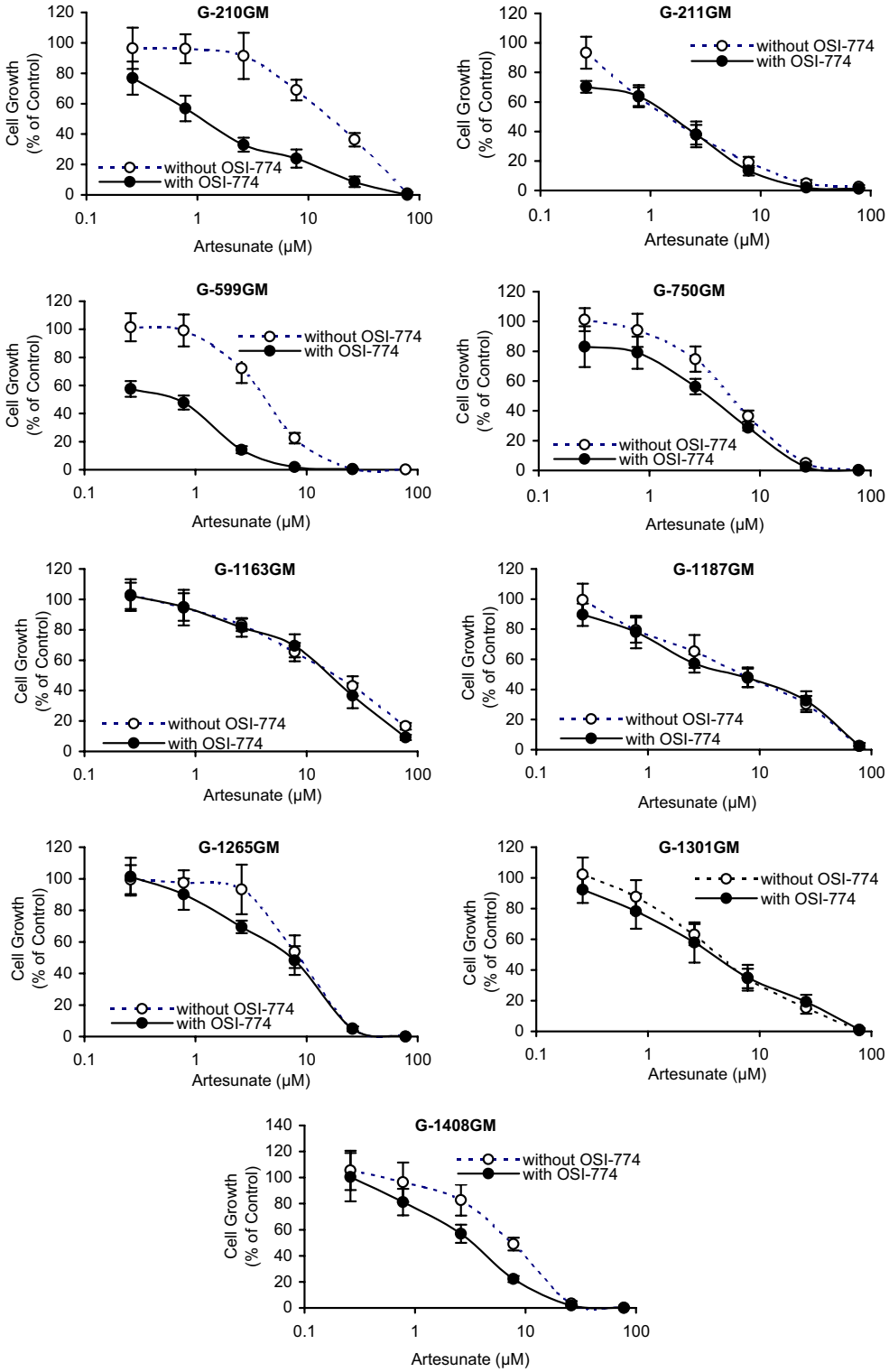

Fig. 3. Combination treatment of nine non-transduced glioblastoma cell lines with ART and OSI-774 assessed by the growth inhibition assay. For details see legend of Fig. 2.

These genomic imbalances of the GBM cell lines were then investigated by hierarchical cluster analysis and clustered image mapping in order to detect genomic profiles of imbalances that predict sensitivity or resistance to ART and OSI-774. The upper dendrogram in Fig. 6 could be divided into two major clusters (clusters A and B), and the dendrogram on the right into three major clusters (clusters 1, 2, and 3). First, we examined whether the distribution of genomic imbalances was different between the clusters with statistical significance. As shown in Table 2, genomic

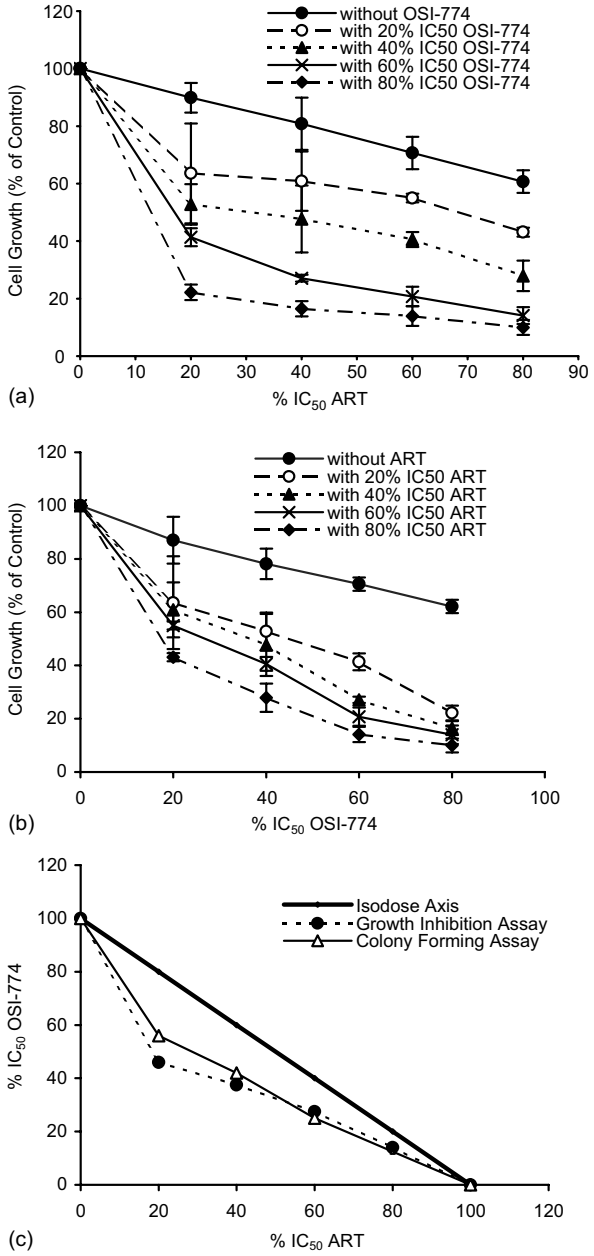

Fig. 4. Isobologram analysis (50% isodose) of ART and OSI-774 combination treatments. Growth inhibition after exposure to serial dilutions of both drugs plotted against (a) OSI-774 or (b) ART. The isobolographic plot (c) shows the IC_{50} values of combined treatments. The diagonal line represents additivity. Data points that fall to the left of this line indicate supra-additivity or synergy. Data represent mean ± S.D. of four measurements.

imbalances of clusters 1 and 3 of the dendrogram on the right (Fig. 6) were differentially distributed between clusters A and B of the upper dendrogram ($P = 0.00484$; χ^2 test), while genomic imbalances of cluster 2 were not. Then, we correlated the two clusters on the top of Fig. 6 with the IC_{50} values for ART and OSI-774 that were not included into the cluster analysis beforehand (Table 2). The distribution of sensitive and resistant GBM cell lines was significantly different among these two clusters ($P = 0.02845$). At a cut-off IC_{50} value of 5 μM, cluster

Table 2
Statistical analysis of genomic imbalances in GBM cell lines subjected to hierarchical cluster analysis in Fig. 5

	Cluster A	Cluster B	Significance
Cluster 1	10	5	$P = 0.00484$[a]
Cluster 2	4	4	
Cluster 3	3	18	
Sensitive (≤5 μM)	4	1	$P = 0.02845$[a]
Resistant (>5 μM)	0	3	

[a] χ^2 test.

B contained cell lines that were more resistant to ART and OSI-774, while cluster A was enriched with more sensitive cell lines. As can be seen in the cluster image map in Fig. 6, the genomic imbalances of cluster 1 (dim(18q22q23), enh(15q14), and enh(14q12)) were more frequently present in the "sensitive" cluster A, whereas the genomic aberrations of cluster 3 (dim(4q22q33), dim(16p12), enh(5p), enh(10q21q24), and enh(2q37)) were more frequently present in the "resistant" cluster B.

4. Discussion

4.1. Additive and supra-additive growth inhibition by ART and OSI-774

In the present investigation, we analyzed the combination treatment of ART and OSI-774 in a panel of 14 GBM cell lines. OSI-774 was applied in a concentration of 1 μM in combination with ART. In a recent phase I study on patients with advanced solid malignancies [22], the average minimal steady state plasma concentration of OSI-774 was 1.2 μg/ml (3 μM). Hence, the concentration of 1 μM that was active in the present investigation is safely within the range of clinically achievable plasma concentrations. The same applies to ART. The IC_{50} values for ART in 14 GBM cell lines ranged from 1.5 to 18.8 μM. OSI-774 modulated ART-induced growth inhibition in these cell lines by reducing the IC_{50} range from 0.6 to 15.8 μM. In clinical anti-malarial studies, peak plasma concentrations of 2640 ± 1800 μg/ml (6.88 ± 4.69 mM) have been achieved upon intravenous application of 2 mg/kg ART [23]. Hence, peak plasma concentrations were two to three orders of magnitude higher than the IC_{50} values for ART in the present study. As the doses of both ART and OSI-774 were well within clinically relevant ranges, the results obtained in this investigation might gain relevance for the inhibition of tumor cell growth in humans.

An *EGFR* gene deletion mutation comprising exons 2–7 conferred resistance to ART, whereas the wild-type *EGFR* gene or *EGFR* with deficient tyrosine kinase activity did not. Unlike wild-type *EGFR*, the gene product of deletion-mutant *EGFR* is constitutively active in a ligand-independent manner [12], indicating that the extent of stimulated EGFR autophosphorylation influences cellular response to

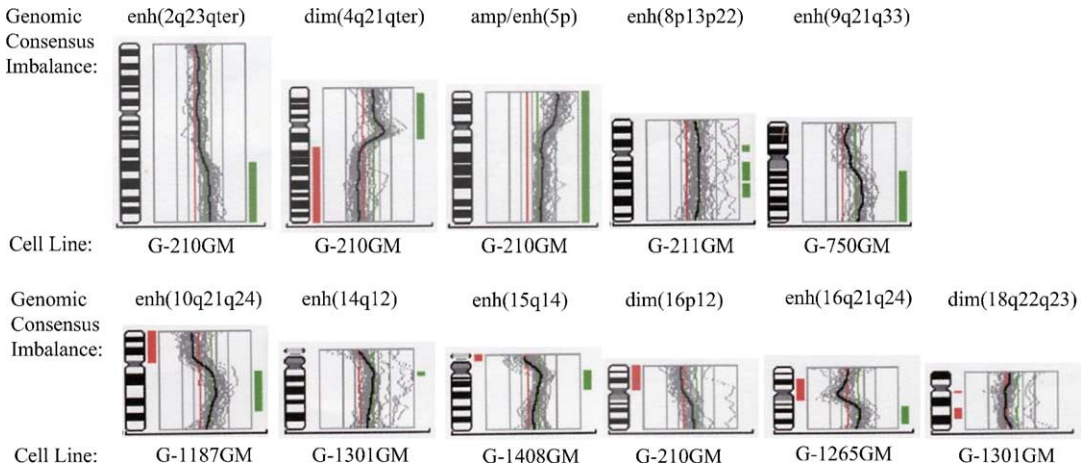

Fig. 5. Representative examples of genomic consensus imbalances obtained by comparative genomic hybridization that correlated with IC_{50} values for ART and OSI-774.

ART. This is also known for other anticancer drugs like cisplatin, doxorubicin, homoharringtonine, paclitaxel, or vincristine [24–26]. As EGFR affects resistance to multiple structurally and functionally unrelated drugs, it can be assumed that *EGFR*-mediated drug resistance may be yet another variant of pleiotropic drug resistance in addition to the classical multidrug resistance phenotypes caused by ATP-binding cassette transporter genes, i.e., *MDR1*, *MRP*, or *BCRP*.

In contrast to treatment with ART alone, we observed that U-87MG.ΔEGFR cells were even more sensitive to treatment with OSI-774 alone than the control cell lines U-87MG and U-87MG.LUX. This may be explained by a strong dependency of ΔEGFR-expressing cells on a permanently high activity of EGFR-downstream signaling pathways. Upon disruption of EGFR pathway signaling by OSI-774 the U-87MG.ΔEGFR cells were more inhibited as the other U-87MG cell lines. This observation fits to recent results showing that OSI-774 acts preferentially on cells with highly malignant phenotypes [1].

Recent studies have demonstrated that EGFR may regulate cellular responses to cytotoxic drugs by regulation of key molecules of apoptosis, e.g., BCL2, BCL-X, MYC, and NFκB1 [27–29] either by activation of transcription factors, i.e., CREB and FOS, or by phosphorylation of target proteins. Roles of EGFR, RAF, AKT, PKC, the

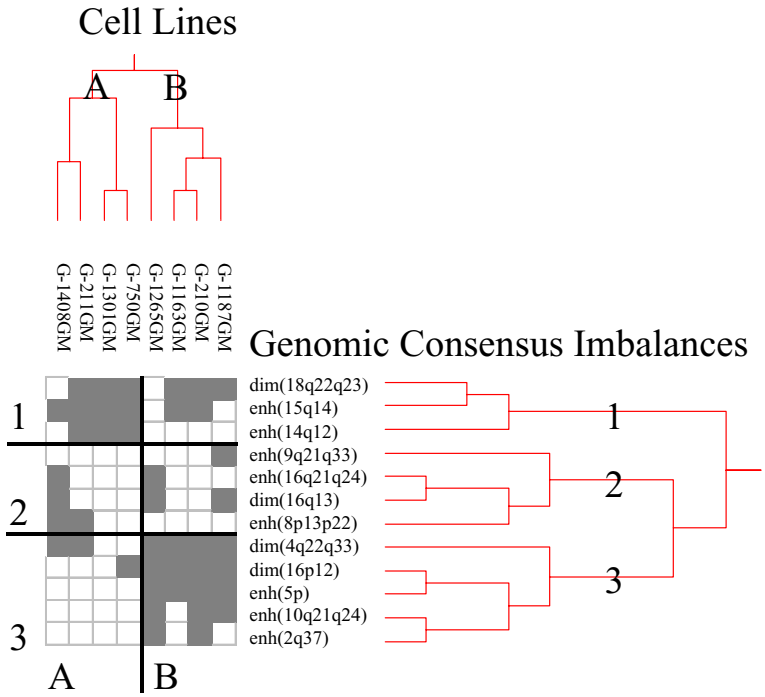

Fig. 6. Dendrograms and clustered image map obtained by hierarchical cluster analysis (complete linkage method). The dendrogram to the right shows the clustering of genomic imbalances (gains or losses) detected by comparative genomic hybridization (see Table 1) and the top dendrogram of GBM cell lines. Light fields indicate 'imbalance not present', and dark fields indicate 'imbalance present'.

Table 3
Genes of genomic imbalances that correlate with IC_{50} values for ART and OSI-774

Genomic imbalance	Gene locus	Symbol	Gene name	Gene function
enh(2q23qter)	2q23	*PKCl*	Protein kinase C λ	Signal transduction; phosphorylation of target proteins
	2q31	*CDCA7*	Cell division cycle associated 7	Proliferation; target gene of c-myc; participation in c-myc-mediated transformation
	2q31	*RAB6C*	*RAB6C*, member of the *RAS* oncogene family	Oncogene; involved in multidrug resistance
	2q33	*ABI-2*	abl-interactor 2	Signal transduction; coordination of cytoplasmic and nuclear functions of ABL1 tyrosine kinase
	2q33	*FZD7*	Frizzled homologue 7 (Drosophila)	Signal transduction; wingless-type (wnt)-receptor that signals for adenenomatous polyposis of the colon (APC) tumor suppressor and β-catenin
	2q35	*CDK5R2*	Cyclin-dependent kinase 5, regulatory subunit 2 (p39)	Proliferation; neuronal cyclin-dependent kinase 5 activator isoform
dim(4q21qter)	4q27	*MAD2L1 (MAD2)*	Mitotic arrest deficient 2, yeast *S. cerevisiae*, human homolog like-1	Proliferation; monitoring of accurate chromosome segregation
	4q21q23	*JNK3 (MAPK10)*	c-jun N-terminal kinase 3 (mitogen-activated kinase 10)	Signal transduction; mediation of immediate-early gene expression
	4q23q24	*NFKB1*	Nuclear factor κB 1	Apoptosis, tumorigenesis; regulation of gene expression
	4q32q32	*HCC2*	Hepatocellular carcinoma 2	Oncogene in hepatocellular carcinomas
amp/enh(5p)	5p13.3p13.1	*GDNF*	Glial cell line-derived neurotrophic factor	Apoptosis; interaction between ret and ras pathways
	5p14p12	*GHR*	Growth hormone receptor	Proliferation; receptor activation leads to synthesis of insulin-like growth factor 1 (IGF1)
enh(8p13p22)	8p21.1	*GSR*	Glutathione reductase	Chemoprotection; catalysis of oxidized glutathione and $NADP^+$ to reduced Glutathione disulfide and NADPH + H^+; enzyme of the antioxidant glutathione redox cycle
enh(9q21q33)	9q22	*TEC*	tec protein tyrosine kinase	Signal transduction; activation of growth and differentiation processes
	9q22	*SYK*	Spleen tyrosine kinase	Putative tumor suppressor; non-receptor type protein-tyrosine kinase
	9q34.3	*NUP214*	Nuclear pore complex protein 241 kDa	Proliferation; role in nucleocytoplasmic transport processes and cell cycle progression
	9q22.3	*PTCH1*	Patched (Drosophila)	Signal transduction; repression of cell proliferation, role in DNA maintenance, repair and/or replication
enh(10q21q24)	10q24	*NFKB2*	Nuclear factor κB2	Regulation of genes involved in cell to cell interaction, spreading of primary pathogenic signals, initiation or acceleration of tumorigenesis
	10q23.3	*PTEN*	Phosphatase and tensin homologue	Tumor suppressor; negative regulator of the phosphatidylinositol 3-kinase (PI3K)/AKT pathway
	10q24	*LGI1*	Leucine-rich gene glioma inactivated 1	Tumor suppressor rearranged and downregulated in malignant brain tumors; involvement in malignant progression of glial tumors
	10q24q25	*MXI1*	Max interacting protein 1	Tumor suppressor; suppression of cell growth by competition with myc for interaction with max
	10q21.1q22.1	*EGR2*	Early growth response 2	Proliferation; targeting of proteins required for synthesis of normal myelin lipids

Table 3 (*Continued*)

Genomic imbalance	Gene locus	Symbol	Gene name	Gene function
	10q24.1	*APT1 (TNFRSF6)*	Apoptosis antigen 1 (Fas, APO-1, CD95) (tumor necrosis factor receptor superfamily member 6)	Apoptosis; activator of an extrinsic apoptotic signaling pathway
enh(14q12)	14q11q12	*DAD1*	Defender against cell death 1	Apoptosis; inhibitor of programmed cell death
enh(15q14)	15q14	*AF15q14*	ALL1 fused gene from 15q14	Oncogene in acute lymphoblastic leukemia
dim(16p12)	16p12.2	*PKCB1*	Protein kinase C β 1	Signal transduction; phosphorylation of many cellular proteins after activation by diacyglycerol and tumor promoters (phorbol esters)
	16p12p11.2	*ASC*	Apoptosis-associated speck-like protein containing a caspase recruitment domain (CARD)	Apoptosis; promotion of caspase-dependent apoptosis induced by anticancer drugs
enh(16q21q24)	16q22	*CBFb (PEBP2b)*	Subunit b of core binding factor (polyomavirus enhancer binding protein 2b)	Transcription factor; core-binding factor subunit b (CBFb) increases binding of CFBa to DNA; involved in leukemogenesis
	16q24.1q24.3	*WFDC1*	Whey acidic protein (WAP) four-disulfide core domain 1	Putative tumor suppressor; protease inhibitor that inhibits growth and maintains tissue homeostasis
	16q22.1	*DIA4 (NQO1)*	DT-diaphorase 4, NAD(P)H: quinone oxidoreductase 1	Chemoprotection; protection from oxidative challenge and preclusion of generation of reactive oxygen radicals
	16q22.1	*CDH1*	Cadherin 1, E-cadherin	Cellular adhesion; CDH1 and Drosophila SNAIL 1 homologue (SNAI1) transcription factor regulate cell migration in tumor invasion and metastasis
dim(18q22q23)	18q22qter	*TGFBRE*	Transforming growth factor β1 response element	Acquisition of cellular resistance to growth inhibitors, such as TGFB1

Gene information was taken from the OMIM and LocusLink databases, National Cancer Institute, USA (http://www.ncbi.nlm.nih.gov/Omim/, http://www.ncbi.nlm.nih.gov/LocusLink/), from the GeneCard database of the Weizman Institute of Science, Rehovot, Israel (http://bioinfo.weizmann.ac.il/cards/index.html), and from the Genome Database of the Human Genome Project (http://www.gdb.org).

BCL2 protein family, NFκB1, and FOS for resistance to established anti-tumor drugs have been demonstrated previously [3,30–32], suggesting that downstream pathways of *EGFR* signaling may also contribute to the response of tumor cells to ART.

The fact that the over-expression of constitutively activated EGFR decreases sensitivity of GBM to ART renders inhibitors of EGFR attractive candidates for combination treatments with this compound. In vitro and in vivo studies have demonstrated additive to synergistic effects of small molecule tyrosine kinase inhibitors or monoclonal antibodies against EGFR in combination with established anticancer drugs [5,6]. This has also been observed for antibodies against a closely related gene of *EGFR*, *HER2*, and cytostatic drugs [33]. Comparable results have been found for OSI-774 in combination with established anticancer drugs [34]. In the present investigation with a panel of GBM cell lines, we found that OSI-774 plus ART produced additive and supra-additive inhibition in cell growth and colony forming assays. These results support the hypothesis of Mendelsohn and Fan [35] that chemotherapy converts EFGR ligands from growth factors to survival factors. Repression of EGFR protein function by specific inhibitors in combination with cytotoxic drugs may cause irreversible cell damage that leads to apoptosis.

4.2. Comparative genomic hybridization and hierarchical cluster analysis

All of the non-transduced cell lines examined contained an enhancement of the short arm of chromosome 7 where the *EGFR* gene is located and expressed or over-expressed *EGFR* mRNA and protein to a different extent [21,36]. Although OSI-774 inhibits downstream EGFR signaling in a specific manner, the response of our panel of GBM cell lines to ART and OSI-774 is, however, not strictly determined by EGFR expression, and other factors may also contribute to the tumor cells' responses to these drugs.

The comparative genomic hybridization technique was used to detect all genetic imbalances of each cell line at the genomic level in one single hybridization experiment. This approach allows to correlate the presence of genomic

aberrations with the individual IC_{50} values for ART and OSI-774 in these cell lines and thereby to identify genomic regions that are associated with drug sensitivity and resistance. The genes located at these genomic loci (Table 3) may influence the action of ART and OSI-774 in the individual cell lines. The genes belong to classes of different biological functions, e.g., genes involved in apoptosis, proliferation, signal transduction, or xenobiotic detoxification as well as oncogenes and tumor suppressor genes. Some of these genes have been already shown previously to cause resistance to established anticancer drugs, i.e., *GSR*, *PKCB1*, *NFKB1*, *TNFRSF6* (CD95), and *RAB6C* [31,37–40], some of them being targets of EGFR signaling pathways as discussed above. By means of hierarchical cluster analysis we have shown here that it is indeed possible to predict sensitivity or resistance of glioblastoma cell lines to ART and OSI-774 based on their genomic imbalances. Consequently, certain genes allocated to the respective genomic loci may contribute to drug sensitivity and resistance. In how far the genes identified by our approach are causally related to sensitivity or resistance to ART and OSI-774 requires further investigation.

In summary, we have demonstrated that the combination of ART and OSI-774 provoked additive to supra-additive growth inhibition in 14 GBM cell lines. Cells transduced with deletion–mutation-driven constitutive activation of EGFR were highly sensitive to ART and OSI-774. Furthermore, we observed a relationship between genetic alterations and sensitivity to ART and OSI-774 in non-transduced cell lines. Our results warrants further studies to dissect the molecular architecture that determines sensitivity and resistance of tumor cells to ART and OSI-774 in more detail.

Acknowledgments

T.R. was funded by the German-Mexican Exchange Program of the *Deutsche Forschungsgemeinschaft* (given to E.G.) and Conacyt, Mexico. The project was additionally supported by an intramural grant of the University of Göttingen (given to M.-E.H.). We thank Karen Thoma for skillful technical assistance.

References

[1] Halatsch M-E, Schmidt U, Bötefür IC, Holland JF, Ohnuma T. Marked inhibition of glioblastoma target cell tumorigenicity in vitro by retrovirus-mediated transfer of a hairpin ribozyme against deletion-mutant epidermal growth factor receptor messenger RNA. J Neurosurg 2000; 92:297–305.

[2] Arteaga CL. Epidermal growth factor receptor dependence in human tumors: more than just expression? Oncologist 2002;7(Suppl 4):31–9.

[3] Navolanic PM, Steelman LS, McCubrey JA. EGFR signaling and its association with breast cancer development and resistance to chemotherapy (review). Int J Oncol 2003;22:237–52.

[4] Modi S, Seidman AD. An update on epidermal growth factor receptor inhibitors. Curr Oncol Rep 2002;4:47–55.

[5] Efferth T, Volm M. Antibody-directed therapy of multidrug-resistant tumor cells. Med Oncol Tumor Pharmacother 1992;9:11–9.

[6] Raben D, Helfrich BA, Chan D, Johnson G, Brunn Jr PA. ZD1839, a selective epidermal growth factor receptor tyrosine kinase inhibitor, alone and in combination with radiation and chemotherapy as a new therapeutic strategy in non-small cell lung cancer. Semin Oncol 2002; 29(4):37–46.

[7] Moyer JD, Barbacci EG, Iwata KK, Arnold L, Boman B, Cunningham A, et al. Induction of apoptosis and cell cycle arrest by CP-358,774, an inhibitor of epidermal growth factor receptor tyrosine kinase. Cancer Res 1997;57:4838–48.

[8] Norman P. OSI-774 OSI pharmaceuticals. Curr Opin Investig Drugs 2001;2:298–304.

[9] Halatsch M-E, Gehrke EE, Vougioukas VI, Bötefür IC, Al-Bohrani F, Efferth T, et al. Inverse correlation of epidermal growth factor receptor (EGFR) mRNA induction and suppression of anchorage-independent growth by OSI-774, an EGFR tyrosine kinase inhibitor, in glioblastoma multiforme cell lines. J Neurosurg 2004;100:523–33.

[10] Efferth T, Dunstan H, Sauerbrey A, Miyachi H, Chitambar CR. The anti-malarial artesunate is also active against cancer. Int J Oncol 2001; 18:767–73.

[11] Efferth T, Sauerbrey A, Olbrich A, Gebhart E, Rauch P, Weber HO, et al. Molecular modes of action of artesunate in tumor cells. Mol Pharmacol 2003;64:382–94.

[12] Huang H-JS, Nagane M, Klingbeil CK, Lin H, Nishikawa R, Ji XD, et al. The enhanced tumorigenic activity of a mutant epidermal growth factor receptor common in human cancers is mediated by threshold levels of constitutive tyrosine phosphorylation and unattenuated signaling. J Biol Chem 1997;272:2927–35.

[13] Nagane M, Coufal F, Lin H, Bogler O, Cavenee WK, Huang HJ. A common mutant epidermal growth factor receptor confers enhanced tumorigenicity on human glioblastoma cells by increasing proliferation and reducing apoptosis. Cancer Res 1996;56:5079–86.

[14] Steel GG, Peckham MJ. Exploitable mechanisms in combined radiotherapy-chemotherapy: the concept of additivity. Int J Radiat Oncol Biol Phys 1979;5:85–91.

[15] Berenbaum MC. Criteria for analyzing interactions between biologically active agents. Adv Cancer Res 1981;35:269–335.

[16] Wolff E, Liehr T, Vorderwülbecke U, Tulusan AH, Husslein EM, Gebhart E. Frequent gains and losses of specific chromosome segments in human ovarian carcinomas shown by comparative genomic hybridization. Int J Oncol 1997;11:19–23.

[17] Gebhart E, Verdorfer I, Saul W, Trautmann U, Brecevic L. Delimiting the use of comparative genomic hybridization in human myeloid neoplastic disorders. Int J Oncol 2000;16:1099–105.

[18] Verdorfer I, Brecevic L, Saul W, Schenker B, Kirsch M, Trautmann U, et al. Comparative genomic hybridization-aided unraveling of complex karyotypes in human hematopoietic neoplasias. Cancer Genet Cytogenet 2001;124:1–6.

[19] Desper R, Jiang F, Kallioniemi O, Moch H, Papadimitriou CH, Schäffer AA. Inferring tree models for oncogenesis from comparative genomic hybridization data. J Comput Biol 1999;6:37–51.

[20] Efferth T, Verdorfer I, Miyachi H, Sauerbrey A, Drexler HG, Chitambar CR, et al. Genomic imbalances in drug-resistant T-cell acute lymphoblastic CEM leukemia cell lines. Blood Cells Mol Dis 2002; 29:1–13.

[21] Ramirez T, Thoma K, Taja-Chayeb L, Efferth T, Herrera LA, Halatsch ME, et al. Specific patterns of DNA copy number gains and losses in eight new glioblastoma multiforme cell lines. Int J Oncol 2003;23: 453–60.

[22] Hildalgo M, Siu LL, Nemunaitis J, Rizzo J, Hammond LA, Takimoto C, et al. Phase I and pharmacological study of OSI-774, an epidermal growth factor receptor tyrosine kinase inhibitor, in patients with advanced solid malignancies. J Clin Oncol 2001;19:3267–79.

[23] Batty KT, Davis TM, Thu LT, Binh TQ, Anh TK, Ilett KF. Selective high-performance liquid chromatographic determination of artesunate and alpha- and beta-dihydroartemisinin in patients with falciparum malaria. J Chromatogr B Biomed Appl 1996;677:345–50.
[24] Dickstein BM, Wosikowski K, Bates SE. Increased resistance to cytotoxic agents in ZR75B human breast cancer cells transfected with epidermal growth factor receptor. Mol Cell Endocrinol 1995;110: 205–11.
[25] Nagane M, Levitzki A, Gazit A, Cavenee WK, Huang H-JS. Drug resistance of human glioblastoma cells conferred by a tumor-specific mutant epidermal growth factor receptor through modulation of BCL-X_L and caspase-3-like proteases. Proc Natl Acad Sci USA 1998;95: 5724–9.
[26] Efferth T, Sauerbrey A, Halatsch M-E, Ross DD, Gebhart E. Molecular modes of action of cephalotaxine and homoharringtonine from the coniferous tree *Cephalotaxus hainanensis* in human tumor cell lines. Naunyn-Schmiedeberg's Arch Pharmacol 2003;367:56–67.
[27] Catz SD, Johnson JL. Transcriptional regulation of bcl-2 by nuclear factor kappa B and its significance in prostate cancer. Oncogene 2001;20:7342–51.
[28] Arcinas M, Heckman CA, Mehew JW, Boxer LM. Molecular mechanisms of transcriptional control of bcl-2 and c-myc in follicular and transformed lymphoma. Cancer Res 2001;61:5202–6.
[29] Glasgow JN, Qiu J, Rassin D, Grafe M, Wood T, Perez-Pol JR. Transcriptional regulation of the BCL-X gene by NF-κB is an element of hypoxic responses in the rat brain. Neurochem Res 2001;26:647–59.
[30] Boldogh I, Ramana CV, Chen Z, Biswas T, Hazra TK, Grosch S, et al. Regulation of expression of the DNA repair gene O^6-methylguanine-DNA methyltransferase via protein kinase C-mediated signaling. Cancer Res 1998;58:3950–6.
[31] Tergaonkar V, Pando M, Vafa O, Wahl G, Verma I. p53 stabilization is decreased upon NFκB activation: a role for NFκB in acquisition of resistance to chemotherapy. Cancer Cell 2002;1:493–503.
[32] Davis JM, Navolanic PM, Weinstein-Oppenheimer CR, Steelman LS, Hu W, Konopleya M, et al. Raf-1 and bcl-2 induce distinct and common pathways that contribute to breast cancer drug resistance. Clin Cancer Res 2003;9:1161–670.
[33] Toma S, Colucci L, Scarabelli L, Scaramuccia A, Amionite L, Bettsa PG, et al. Synergistic effect of the anti-HER-2/neu antibody and cisplatin in immortalized and primary mesothelioma cell lines. J Cell Physiol 2002;193:37–41.
[34] Pollack VA, Savage DM, Baker DA, Tsaparikos KE, Sloan DE, Moyer JD, et al. Inhibition of epidermal growth factor receptor-associated tyrosine phosphorylation in human carcinomas with CP-358,774: dynamics of receptor inhibition in situ and antitumor effects in athymic mice. J Pharmacol Exp Ther 1999;291:739–48.
[35] Mendelsohn J, Fan Z. Epidermal growth factor receptor family and chemosensitization. J Natl Cancer Inst 1997;89:341–3.
[36] Halatsch M-E, Gehrke EE, Al-Borhani F, Efferth T, Werner C, Nomikos P, et al. EGFR but not PDGFR-β expression correlates to the antiproliferative effect of growth factor withdrawal in glioblastoma multiforme cell lines. Anticancer Res 2003;23:2315–20.
[37] Fan D, Fidler IJ, Ward NE, Seid C, Earnest LE, Housey GM, et al. Stable expression of a cDNA encoding rat brain protein kinase C-beta I confers a multidrug-resistant phenotype on rat fibroblasts. Anticancer Res 1992;12:661–7.
[38] Hao XY, Bergh J, Brodin O, Hellman U, Mannervik B. Acquired resistance to cisplatin and doxorubicin in a small cell lung cancer cell line is correlated to elevated expression of glutathione-linked detoxification enzymes. Carcinogenesis 1994;15:1167–73.
[39] Friesen C, Fulda S, Debatin KM. Deficient activation of the CD95 (APO-1/Fas) system in drug-resistant cells. Leukemia 1997;11: 1833–41.
[40] Shan J, Mason JM, Yuan L, Barcia M, Porti D, Calabro A, et al. Rab6C, a new member of the rab gene family, is involved in drug resistance in MCF76/AdrR cells. Gene 2000;257:67–75.